Estimating Fractional Cover of Grassland Components from Two Satellite Remote Sensing Sensors

ZHANG Yongqin[1], SMITH Anne M. [1], HILL Michael J.[2]

[1] Agriculture and Agri-Food Canada, Lethbridge, Alberta, Canada-(yongqin.zhang, anne.smith)@agr.gc.ca
[2] The University of North Dakota, Grand Forks, North Dakota, USA-hillmj@aero.und.edu

Abstract

In this study, the fractional cover (*f*) of three grassland components (photosynthetic vegetation (PV), non-photosynthetic vegetation (NPV), and background (B)) were estimated using Landsat 5 and CHRIS/Proba sensors. In 2009, a field campaign was carried out at three sites on the mixed prairie of southern Alberta, Canada to collect *in situ* measurements of fractional cover. Landsat 5 and CHRIS/Proba images were acquired near the same time as the ground measurements. The *f*PV was found to be closely related to the Modified Transformed Vegetation Indexes 1 and 2 (MTVI1, MTVI2; R^2 0.72 and 0.76) calculated from Landsat imagery. Narrow band versions of these and two other narrow band indices, the Red-edge Index (RE) and the Transformed Chlorophyll Absorption in Reflectance Index/Optimized Soil-Adjusted Vegetation Index (TCARI/OSAVI)), derived from nadir CHRIS imagery were also reasonable predictors of *f*PV. The estimates of non-photosynthetic vegetation were poor using these indices. A soil adjusted vegetation index, the Normalized Difference Senescent Vegetation Index derived from Landsat 5 produced a reasonable relationship with NPV ground cover (R^2 0.70; RMSE 3.52%). Estimation of *f*B from 100-(*f*PV+*f*NPV) consequently gave a similar reasonable relationship (R^2 of 0.71~ 0.82 and RMSE of 5.57~7.06%). The results showed that *f*PV and *f*NPV of mixed prairie rangeland could be estimated with an RMSE of 4-6% using Landsat-derived vegetation indices. Such estimates of *f* could become a critical input to more comprehensive estimation of grassland biomass and growth rates in Alberta rangelands.

Key words: grassland ecosystem, remote sensing, fractional cover, vegetation, background

1 INTRODUCTION

Grasslands play a vital ecological and environmental role in global carbon balance and climate change. In the prairie provinces of Canada, grasslands occupy approximately 25 M ha of the land base (Statistics Canada 2006) and provide a valuable resource to the multi-billion dollar cattle industry. In managing grasslands, maintenance of adequate vegetation cover, both photosynthetic and non-photosynthetic, prevents land erosion by minimizing soil exposure and potential erosion by wind and water. The amount of photosynthetic vegetation (PV) provides an estimate of the net primary productivity of the grassland ecosystems. The non-photosynthetic vegetation (NPV), often called litter, plays an important role in moderating heat fluxes and contributing to nutrient cycling, water retention, and site stability. Thus, estimates of the fractional ground cover (*f*) of grasslands, namely PV, NPV and B, are important for evaluating productivity and health of grassland ecosystems.

In recent years, remote sensing technology has been applied for estimating the fractional cover of arid grasslands and savannah ecosystems (Asner and Heidebrecht, 2003; Marsett et al. 2006; Guerschman et al., 2009). To date no similar studies have been conducted in Alberta. Annually, net primary productivity of Alberta grasslands is measured in the fall by manual clipping at reference sites across the province (Anon, 2004). The clippings are used as an indicator of (a) the effects of annual climate fluctuations on primary forage productivity; (b) the effects of forest succession on primary forage productivity in grazed and ungrazed situations; and (c) to determine if there are any differences in long-term forage productivity between different plant community types. The reference sites are small and of limited numbers. Remote sensing offers a potential tool to replace the manual clippings and/or spatially extrapolate the ground-based measurements over the landscape which contains variable site types. In this study, we explored (1) a method to derive fractional cover of grassland components using broad band multispectral imagery from the Landsat satellite and (2) the potential to improve estimates of *f* in grasslands using narrow band hyperspectral imagery acquired by the Compact High Resolution Imaging Spectrometer (CHRIS) on board the Proba-1 satellite.

2 MATERIALS AND METHODS

2.1 Study sites

Three test sites, Twin River (49.02° N, 112.34°W), Aden (49.13° N, 111.29° W) and Cressday (49.25° N, 110.23°W) were selected for this study. The sites represent a gradient in potential production evident from the west to east in the southern region of Alberta, Canada (Figure 1). At each site, five 140 m long transects were established and sampling points set up every 10 m for a total of 15 sampling points per transect and 75 per site.

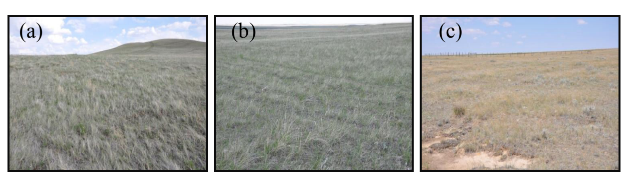

Figure1: Three test sites used in this study (a) Twin River; (b) Aden and (c) Cressday.

2.2 Field data collection and analysis

A field campaign was conducted in early July 2009 to coincide with the anticipated time of peak grass production (Table 1). Digital hemispherical photos were taken at each sampling point to estimate percent ground cover of the various grasslands components using a Nikon D90 digital camera. All photographs were taken 1.35 m above the ground at a nadir look angle. The photographs were analyzed using an unsupervised classification algorithm ISODATA in ENVI* software. After classifying the photographs into 14 subclasses, the subclasses were combined to derive the percent cover of PV (green grass, forbs and shrubs), NPV (senescent grass, forbs and shrubs) and B (bare soil and lichens). This method of estimating ground cover using hemispherical photographs was previous validated by Zhang et al. (2010). The mean percent cover values per transect was calculated.

2.3 Satellite data acquisition and processing

Landsat TM 5 images with 30 m spatial resolution were obtained from US Geological Survey (Table 1). The six bands within the imagery for each date were radiometrically calibrated and atmospherically corrected to derive the surface reflectance images using the FLAASH module in ENVI.

Mode 1 CHRIS imagery comprising 62 spectral bands over the range of 405-1005 nm in up to five look angles (0, ±36, ±55^{o}) at 34 m spatial resolution was acquired for the three test sites (Table 1). The images were processed to surface reflectance after noise reduction, cloud screening, and atmospheric correction using BEAM software+. All surface reflectance images were geometrically corrected. Only the nadir look CHRIS reflectance images were analyzed in this study. A 3*3 pixel window was centered over each transect and the reflectance value from the central pixel extracted. This provides 5 observations per site and 15 in total.

Table 1: Time of the field measurements and image acquisition

Site	Field Measurement	CHRIS	Landsat
Twin River	July 6 and 7	June 27	June 28
Aden	July 3 and 8	June 25	June 28
Cressday	July 2 and 3	June 24	July 23

2.4 Estimating ground fractional cover from Landsat imagery

The mean fractional cover of the three grassland components, PV, NPV, and B in each transect were derived using a variety of vegetation indices.

2.4.1 Photosynthetic vegetation cover

A number of vegetation indices, which use a combination of visible and near-infrared (NIR) reflectance were derived to estimate *f*PV. The vegetation indices investigated included: the Normalised Difference Vegetation Index (NDVI) (Rouse et al. 1974)

$$(R_{NIR} - R_{red})/(R_{NIR} + R_{red}) \quad (1)$$

The Modified Transformed Vegetation Index 1 (MTVI 1) (Haboudane et al. 2004):

$$1.2[1.2(R_{NIR} - R_{green}) - 2.5(R_{red} - R_{green})] \quad (2)$$

The Modified Transformed Vegetation Index 2 (MTVI 2) (Haboudane et al. 2004):

$$\frac{1.5[1.2(R_{NIR} - R_{green}) - 2.5(R_{red} - R_{green})]}{\sqrt{2(R_{NIR}+1)^2 - (6R_{NIR} - 5\sqrt{R_{red}}) - 0.5}} \quad (3)$$

In each equation R is reflectance and the subscript indicates the wavelength. The reflectance values in bands 2, 3 and 4 from the Landsat images were used to represent the green, red and NIR reflectance values, respectively.

2.4.2 Non-photosynthetic vegetation cover

The Normalized Difference Senescent Vegetation Index (NDSVI) which uses the shortwave infrared (SWIR) bands (1650 nm, Landsat band 5) and red (Landsat band 3) was derived to estimate *f*NPV (Marsett et al., 2006):

$$(R_{SWIR} - R_{red})/(R_{SWIR} + R_{red}) \quad (4)$$

2.4.3 Grassland background cover

The fractional cover of background (*f*B) was derived based on the estimation of photosynthetic and non-photosynthetic vegetation percent cover:

$$fB = 100 - (fPV + fNPV) \quad (5)$$

2.5. Estimating ground fractional cover from CHRIS imagery

As with the Landsat imagery, the NDVI, MTVI1 and MTVI2 vegetation indices (equations 1-3) were derived. The narrow bands centred on 551, 672 and 800 nm were selected to represent the green, red and NIR reflectance respectively. In addition two other vegetation indices were calculated: the Transformed Chlorophyll Absorption in Reflectance Index/Optimized Soil-Adjusted Vegetation Index (TCARI/OSAVI) (Haboudane et al. 2002):

$$\frac{3[(R_{703} - R_{672}) - 0.2(R_{703} - R_{551})(R_{703}/R_{672})}{(1+0.16)(R_{800} - R_{670})/(R_{800} + R_{670} + 0.16)} \quad (6)$$

and the Red-edge index (RE) (Zarco-Tejada et al. 2001):

$$R_{709}/R_{748} \quad (7)$$

2.6. Statistical analysis

Regression analyses were conducted to evaluate the relationship between *f*PV, *f*NPV and *f*B from ground measurements, and the values derived from the various indices. The Root Mean Square Error (RMSE) was also calculated:

$$RMSE = \sqrt{\frac{1}{n}\sum_{i=1}^{n}(x_i - y_i)^2} \quad (8)$$

where x_i is the percent cover from the digital hemispherical photographs, y_i is the percent cover predicted from the satellite imagery, and n is the number of sampling points

3 RESULTS

3.1. Ground estimates of grassland fractional cover

**ITT; + Obtained from European Space Agency*

The three selected test sites showed a wide dynamic range in the fractional cover of the various grassland components (Figure 2). The Twin River site demonstrated the highest *f*PV and *f*NPV amongst the three sites, with a mean of 45 and 30% respectively. The Aden and Cressday sites had very similar *f*PV with means of 29 and 28% respectively, and small difference in *f*NPV, 25 and 17% respectively. The most abundant *f*B was found at Cressday (55%), followed by Aden (46%). The Twin River site showed the least *f*B (25%).

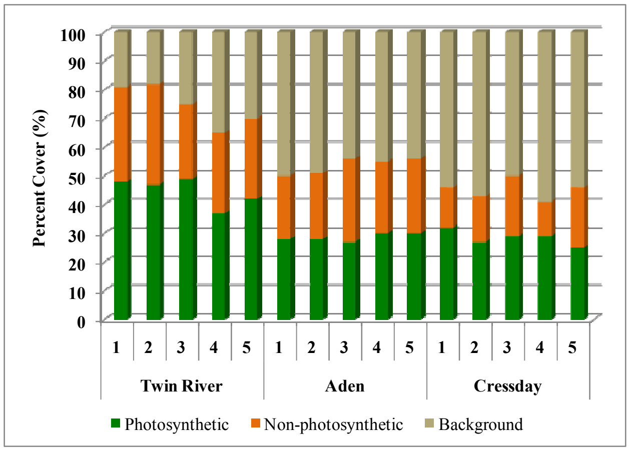

Figure 2: Mean percent ground cover of PV, NPV and B for each of the five transects at the three study sites.

3.2 Estimation of fractional cover of grassland components using Landsat

The MTVI1, MTVI2 both proved more effective in estimating *f*PV, compared to the more widely used NDVI (Table 2). The MTVV1 andMTVI2 explained 76 and 72% of the variation respectively compared to 55% in the case of the NDVI. The RMSE was also lower, 4.03 and 4.30% with the MTVI1 and MTVI2 respectively compared to 5.71% with the NDVI.

Table 2: The relationship between fractional cover of photosynthetic vegetation estimated using Landsat derived vegetation indices and field measurements.

Vegetation index	Equation of correlation*	R^2	RMSE (%)
NDVI	Y=78.55X+3.24	0.55	5.71
MTVI1	Y=143.40X+10.04	0.76	4.03
MTVI2	Y=138.57X+12.11	0.72	4.30

*X denotes vegetation index, Y denotes the percent cover of photosynthetic vegetation and R^2 is the coefficient of determination.

The NDSVI and *f*NPV showed a strong correlation (Figure 3), with non-photosynthetic vegetation cover predicted with an R^2 of 0.70 and RMSE 3.52%.

The *f*B was estimated based on *f*PV and *f*NPV, where *f*PV determines the accuracy of *f*B estimation. It is not surprising that estimates of ground cover were better when *f*PV was estimated by the MTVI1 and MTVI2 than that by the NDVI (Table 3).

**ITT; + Obtained from European Space Agency*

Using the MTVI11 or MTVI2 to estimate *f*PV 80% or more of the variation in background was accounted for and the RMSE was 5.57 and 5.84% respectively.

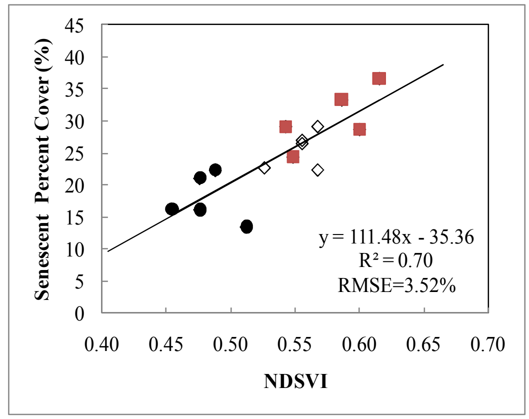

Figure 3: The relationship between NPV percent cover and the Normalized Difference Senescent Vegetation Index (NDSVI) derived from Landsat imagery. The five square makers are for the five transects of the Twin River site, diamonds for the Aden site, and circles for the Cressday site.

Table 3: The relationship between field measurements of *f*B and vegetation indices derived from Landsat.

Vegetation index	Equation of correlation*	R^2	RMSE (%)
NDVI	Y=0.72X+11.71	0.71	7.06
MTVI1	Y=0.82X+7.53	0.82	5.57
MTVI2	Y=0.80X+8.18	0.80	5.84

*X denotes vegetation index, Y denotes the percent cover of non-photosynthetic vegetation and R^2 is the coefficient of determination.

3.3 Estimation of fractional cover of grassland components using CHRIS

The five vegetation indices derived using the narrow-band reflectance data from CHRIS imagery were all closely related to *f*PV (Table 4). The various indices accounted for 65 to 73% of the variation in *f*PV, with RMSE values ranging from 4.37 to 5.81%. Of all the indices tested, the RE provided slightly better estimates than the other indices. To a much lesser extent the five indices related to the *f*NPV (results are not shown here).

Table 4: The relationship between fractional cover of photosynthetic vegetation estimated using CHRIS derived vegetation indices and field measurements.

Vegetation index	Equation of correlation*	R^2	RMSE (%)
NDVI	Y=83.12X-0.68	0.69	5.81
MTVI1	Y=141.04x+9.59	0.65	4.83
MTVI2	Y=129.97x+12.98	0.65	4.79
TCARI/OSAVI	Y=-185.10X+84.76	0.70	4.60
RE	Y=66.58X-59.21	0.73	4.37

*X denotes vegetation index, Y denotes the percent cover of photosynthetic vegetation and R^2 is the coefficient of determination.

4 DISCUSSION

The results suggest that *f*PV can be reasonably well estimated using vegetation indices derived from Landsat and CHRIS satellite imagery. The MTVI1 and MTVI2 which include wavebands in the green as well as the red and NIR portion of the electromagnetic spectrum performed better than the NDVI regardless of the source of imagery. There was no evidence to indicate that narrow band indices performed better than broad band indices with respect to estimating photosynthetic vegetation.

Vegetation indices using visible and near-infrared reflectance correlated poorly to NPV cover. The NDSVI, which is based on a combination of red and SWIR reflectance from Landsat imagery showed good sensitivity to NPV cover. This index was derived in the arid southwest of the USA with much lower total vegetation cover (Marsett et al. 2006). It is therefore significant that it can be equally useful in a temperate rangeland. As the wavelengths available in CHRIS imagery do not extend into the SWIR, this sensor is less useful for detection of NPV and B.

The fractional cover of background was not estimated directly from the imagery. As a result of the satisfactory estimate of photosynthetic and non-photosynthetic vegetation the soil/lichen background was reasonably estimated.

5 CONCLUSION

The results of this study indicated that information on grassland vegetation cover could be indirectly derived from Landsat imagery in the mixed prairie of southern Alberta. The *f*PV, *f*NPV and *f*B of grasslands could be estimated using a combination of indices derived from the imagery with an RMSE in the range of 4-6%. There appeared to be no advantage in estimating *f*PV using narrow as opposed to broad bands. In order to estimate *f*NPV, information in the SWIR is required. Future work will investigate the benefits of narrow as opposed to broad bands for estimating senescent vegetation in the mixed prairie from airborne hyperspectral imagery.

ACKNOWLEDGEMENT

This research is part of a Canadian Government Related Initiatives Program project funded by the Canadian Space Ageny. The authors also acknowledge Gary Larson, Cathy Kloppenberg, Harriet Dowes, Rachel Carreau and Crystal Spearman for their assistance in collecting the ground data.

REFERENCES

Anon. 2004. Rangeland Reference Area Program for the Province Of Alberta. Alberta Sustainable Resource Development Public Lands and Forests Division. 32 pp.

Asner, G. P., and Heidebrecht, K. B., 2003. Imaging spectroscopy for desertification studies: comparing AVIRIS and EO-1 Hyperion in Argentina drylands. *IEEE Transactions on Geoscience and Remote Sensing* 41: 1283-1296.

Guerschman, J.P., Hill, M., Renzullo, L.J., Barrett, D.J., Marks, A.S., Botha, E.J. 2009. Estimating fractional cover of photosynthetic vegetation, non-photosynthetic vegetation and bare soil in the Australian tropical savanna region upscaling the EO-1 Hyperion and MODIS sensors. *Remote Sensing of Environment* 113: 928-945.

Haboudane, D., Miller, J.R., Tremblay, N., Zarco-Tejada, P.J., Dextraze, L. 2002, Integrated narrow-band vegetation indices for prediction of crop chlorophyll content for application to precision agriculture, *Remote Sensing of Environment* 81: 416-426.

Haboudane, D., Miller, J.R., Pattey, E., Zarco-Tejada, P.J., Strachan, I.B. 2004, Hyperspectral vegetation indices and novel algorithms for predicting green LAI of crop canopies: Modeling and validation in the context of precision agriculture, *Remote Sensing of Environment* 90: 337-352.

Marsett,R.C., Qi, J., Heilman,P., Biedenbender, S.H., Watson, M. C., Amer, S., Weltz,M., Goodrich, D., and Marsett, R., 2006. Remote Sensing for Grassland Management in the Arid Southwest. *Rangeland Ecology and Management* 59:530-540.

Rouse, J. W., Haas, R. H., Schell, J. A., Deering, D. W., & Harlan, J. C., 1974. Monitoring the vernal advancements and retrogradation of natural vegetation. In: NASA/GSFC, Final Report, Greenbelt, MD, USA, pp. 1 –137.

Zhang, Y., Smith, A.M., Larson, G., Kloppenburg, C. 2010. Grassland composition and percent cover estimation using digital hemispherical photographs. In: *Proceedings of Prairie Summit- 31st Canadian Remote Sensing Symposium*. June 1-5. Regina, Saskatchewan, Canada. Pp. 349-352.

Zhang, Y., Smith, A.M. 2010. Estimation of percent ground cover in grasslands from hyperspectral and multi-angle remote sensing imagery. In: *Proceedings of Prairie Summit- 31st Canadian Remote Sensing Symposium*. June 1-5. Regina, Saskatchewan, Canada. Pp. 345-348.

**ITT; [+] Obtained from European Space Agency*